Frontiers in Biomedical Technologies Vol. 13, No. 2 (Spring 2026) 472-491

ORIGINAL ARTICLE

Evaluating the Role of Channel Selection in EEG Anxiety Recognition Rates Utilizing a Chaotic Map

Faezeh Daneshmand-Bahman[1], **Ateke Goshvarpour**[2,3*]

[1] *Department of Biomedical Engineering, Semnan University, Semnan, Iran*

[2] *Health Technology Research Center, Imam Reza International University, Mashhad, Iran*

[3] *Department of Biomedical Engineering, Imam Reza International University, Mashhad, Iran*

*Corresponding Author: Ateke Goshvarpour

Received: 18 August 2024 / Accepted: 26 May 2025

Email: ak_goshvarpour@imamreza.ac.ir

Abstract

Purpose: Today, the human lifestyle has led to an increase in anxiety. Its diagnosis is usually made with questionnaires and by specialist physicians. Recently, objective techniques such as brain-behavior analysis have captivated the attention of scientists for the early detection of this disorder. This study aimed to provide a method for diagnosing anxiety based on electroencephalogram (EEG) signals. Also, presents a new methodology by examining different approaches to brain channel selection and feature extraction based on chaotic maps.

Materials and Methods: The DASPS database was used, containing a 14-channel EEG of 23 people (10 men and 13 women, average age: 30 years). The self-assessment manikin was applied to divide anxiety into 2 and 4 levels. Firstly, four methods were assessed to select the optimal channel; two methods were based on the minimum coefficient of variation, and two methods were based on the maximum relative power. Then, Chebyshev's chaotic map was reconstructed, and two features, including 1) the maximum density and 2) its corresponding sample, were extracted. Finally, the k-Nearest Neighbor (K-NN) and Support Vector Machine (SVM) classifiers were applied.

Results: The results indicated a maximum accuracy of 100% for both two/four-level anxiety detection. In addition, the K-NN outperformed the SVM classifier.

Conclusion: It highlighted the role of some brain channels, as well as the classifier structure, in distinguishing anxiety levels. The outstanding result of the proposed algorithm nominated it as a suitable approach for anxiety detection.

Keywords: Electroencephalography; Anxiety Classification; Chebyshev's Chaotic Map; Channel Selection.

DOI: https://doi.org/10.18502/fbt.v13i2.21945

1. Introduction

Anxiety belongs to a family of mental disorders initially characterized by worry and fear. The DSM-5 (Diagnostic and Statistical Manual of Mental Disorders) categorizes anxiety into separation anxiety disorder, selective mutism, specific phobia, social anxiety disorder (social phobia), panic disorder, panic attack, agoraphobia, Generalized Anxiety Disorder (GAD), substance/medication-induced anxiety disorder, and anxiety disorder due to another medical condition [1]. Anxiety is the most common mental health problem worldwide [2, 3], especially in adolescents [4]. The prevalence of anxiety over 12 months is 18% in the United States [1]. Women are 1.5 to 2 times more likely than men to develop anxiety disorders [5]. It imposes a significant economic burden and impairment on the individual quality of life [6]. Additionally, it has many side effects, including redness, paleness, tremors, sweating, sudden cold and heat throughout the body, palpitations, syncope [7], and the like. In addition, it can simultaneously occur with other disorders, including major depressive disorder, personality disorders, and substance abuse. For treating this disorder, medication and psychotherapy options are used based on the patient's history, disease severity, previous treatments, comorbidities, and the like [5].

For diagnosis, some questionnaires and tests are usually applied, including the Structured Clinical Interview for DSM Disorders (SCID) [8], DSM-5 [1], Composite International Diagnostic Interview (CIDI), Diagnostic Interview Schedule (DIS) [7], Hospital Anxiety and Depression Scale (HADS), State-Trait Anxiety Inventory (STAI), and similar instruments [1]. The problem is that when the symptoms are sufficient and severe, anxiety is diagnosed properly [8]. Since the treatment is done on an outpatient basis without needing hospitalization, clinicians pay less attention to it [7]. On the other hand, the outbreak of Covid 19 disease has increased anxiety among people, especially the medical staff [9]. Consequently, the need for new methods for diagnosing it is more than ever. Recently, the use of Electroencephalogram (EEG) signals has attracted the attention of researchers [10-20] because of its advantages, such as low cost, non-invasiveness, and high time resolution [21].

Recent advances in EEG-based anxiety detection have yielded several noteworthy approaches, as summarized in Table 1. The field has progressed from simple spectral analysis to sophisticated machine learning pipelines incorporating both linear and nonlinear features. However, critical limitations persist in current methodologies, particularly regarding channel selection and feature optimization.

Li *et al.* (2019) evaluated the EEG of 73 students in five brain regions, including Left Temporal (LT), Frontal (F), Occipital (O), Frontal-Central-Parietal (FCP), and Right Temporal (RT), for both open and closed eyes. STAI was used to measure anxiety. Seven temporal features, including mean, Standard Deviation (SD), skewness, median, Mean Absolute Deviation (MAD), Interquartile Range (IQR), and trimmed mean (trim-mean), were extracted. A paired-sample t-test was used to evaluate the differences between open and closed eyes, and correlation was performed to examine the relationship between STAI and temporal features in five brain regions. They found that the mean values, trim-mean, IQR, MAD, and SD are higher for closed-eye than for open-eye. STAI also correlates negatively with MAD, SD, and IQR in the open-eye state in the RT region, whereas it correlates positively with SD in the closed-eye state in the FCP [10].

In a study performed by Baghdadi *et al.* (2019), the EEG of 23 healthy individuals was recorded. Some temporal, spectral, and time-frequency properties were calculated. Time-domain features included Hjorth, Higuchi, and QEEG fractal dimensions. Frequency domain features involved Hilbert-Huang spectrum and Fast Fourier Transform (FFT) based band power. Root Mean Square (RMS) and band power of Discrete Wavelet Transform (DWT) were used as time-frequency measures. The features were applied as input of k-Nearest Neighbor (K-NN), Stacked Sparse Autoencoder (SSAE), and Support Vector Machines (SVM) to classify two and four levels of anxiety. Applying all the features to the SSAE, maximum accuracy of 83.5% and 74.60% were obtained for two and four levels of anxiety, respectively [11]. In the study of Wei *et al.* (2020), a recording of 76 people was performed, and the level of anxiety was measured using the Test Anxiety Scale (TAS) before/after the test. Using TAS, people were divided into low and high anxiety levels. Then, the

Table 1. Comprehensive summary of EEG-based anxiety detection studies

Reference	Sample Size	Key Features	Methodology	Performance	Limitations
[10]	73	Temporal statistics	Correlation analysis	Negative correlation of three features with STAI	Limited to temporal features, no classification
[11]	23	Temporal, spectral, and time-frequency	SSAE, SVM, K-NN	83.5% (binary)	Channel selection absence, no feature selection/reduction
[12]	76	Theta/beta ratio, TAS	Statistical testing	p<0.01	No classification
[16]	65	maximum value, signal sum, signal energy, maximum absolute value, and signal peak-to-peak value	logistic regression, MLP and FR	Accuracy: 87.69% (two-level anxiety) 83.07% (three-level anxiety)	No feature selection
[17]	81	PSD, PLI, entropy	SVM, RF, BP_Bagging	97.83% accuracy	No channel selection
[20]	23	Chebyshev chaotic map features	SVM, K-NN	96.15% accuracy	All channels used

Absolute spectral power for Theta/Beta power Ratio (TBR) was calculated at the frontal, central, and parietal sites. Spearman correlation was used to investigate the relationship between TBR and TAS. Additionally, a two-way ANOVA test was used to evaluate TBR before/after the test and high/low anxiety. The results showed that before the test, TAS had a significant positive correlation with parietal TBR. Also, people with high anxiety levels had higher TBR than low anxiety [12]. The relationship between the severity of depression and anxiety was studied [13] using global EEG connectivity. The signals of 119 people were divided into theta, alpha-1, alpha-2, beta-1, beta-2, and gamma. Then, global connectivity was obtained for each band. Support Vector Regression (SVR) was used to predict the symptoms of depression and anxiety, and Loso was used to validate it. The results showed that global connectivity in the alpha-2 band has a significant positive correlation with anxiety and depression [13]. Bocharov *et al.* (2021) evaluated the EEG of 45 subjects. They examined the relationship between rumination, depression, anxiety, and the Default Mode Network (DMN)/Task-Positive Networks (TPN). The connectivity map was achieved using the seed method, and the relationship was expressed using regression. The results showed that rumination and depression are associated with DMN>TPN in the temporal cortex, and anxiety and depression are associated with TPN> DMN in the anterior cingulate [15]. Arsalan and Majid (2022) conducted a study to classify anxiety into two and three levels. In this study, the signal was recorded from 65 people with a MUSE EEG headband, where the electrodes were placed in TP9, TP10, AF7, and AF8 positions. In the next step, they used a t-test for channel selection for two levels and ANOVA for three levels and concluded that the channels have a statistically significant relationship with the groups. Then, in the feature extraction stage, 5 features, including the maximum value, signal sum, signal energy, maximum absolute value, and signal peak-to-peak value, were extracted and applied to the wrapper algorithm to select the best feature. In the classification stage, three algorithms, including logistic regression, MLP, and FR were used. The results of this study showed an accuracy of 87.69% and 83.07% for classification into two and three levels, respectively [16]. Shen *et al.* (2022) conducted a study to diagnose patients with generalized anxiety disorder (GAD). In the mentioned study, the data of 45 patients with GAD and 36 healthy individuals were used. The features, including Power Spectral Density (PSD), Fuzzy Entropy (FE), and d Phase Lag Index (PLI) were extracted from signals. In the next step, ANOVA was used for statistical evaluation of the data. In the last step, three classifiers, including SVM, Random Forest (RF), and ensemble learning of back propagation neural network based on bagging strategy (BP_Bagging), were used to classify the data into two groups, GAD and healthy. The result of this study showed that by using the proposed method, people with GAD can be diagnosed with an accuracy of 97.83% from healthy people [17]. Al-Ezzi *et al.* (2022) conducted a study to classify Social Anxiety Disorder (SAD) into four levels: normal, low, moderate, and high. To achieve the above goal, they used the data of 88 people who were evenly divided into four groups. Then, Fuzzy Entropy was extracted from the signal and applied to the five classifiers, including K-NN, Linear Discriminant Analysis (LDA), naive Bayes classifier (NBC), decision tree (DT), and SVM. The proposed method showed an accuracy of 86.93% to classify SAD into four levels [18]. Muhammad and Al-Ahmadi (2022) conducted a study to classify anxiety into two and four levels using the DASPS database. In this study, a t-test was used to select the channel at two levels and ANOVA was used for four levels. The results of this channel selection showed that AF3, AF4, P7, P8, FC5, and FC6 channels have a significant relationship with the mentioned groups. Then, features including asymmetry index, rational asymmetry, and mean power were extracted from the expressed channels. In the next step, the wrapper method was used to select features, and finally, five classifications including DT, K-NN, SVM, MLP, and RF were used for classification. The result of this study showed an accuracy of 94.90% and 92.74% for the classification of two and four levels, respectively [19]. Despite the research done in this area, there is still a need to provide more accurate methods to diagnose anxiety. The current study aimed to provide a classification system that detects two or four anxiety levels.

The literature review emphasizes three critical gaps in existing EEG-based anxiety detection research that our study directly targets. First, while numerous studies have explored EEG-based anxiety classification, many either lack systematic channel selection or rely on fixed electrode configurations without person-specific optimization. For instance, while [11] achieved 83.5% accuracy using all channels, their approach did not evaluate channel-specific contributions, potentially obscuring individual variability in neural correlates of anxiety. Similarly, [19] employed group-level channel selection (e.g., AF3, AF4) but did not personalize selections for individual participants, a limitation noted in their work. Second, prior studies often overlook the computational inefficiency of using full-channel EEG data, which is particularly relevant for real-world applications. Although [17] reported high accuracy (97.83%), their method required all channels for feature extraction, increasing computational costs. Our study directly addresses this by introducing a novel optimal channel selection framework that reduces data dimensionality while maintaining classification performance. Third, while nonlinear EEG features (e.g., entropy, fractal dimensions) have shown promise, their combination with personalized channel selection remains underexplored. For example, [14] used nonlinear features like Lyapunov exponents but did not integrate them with channel optimization. Our work bridges this gap by pairing Chebyshev chaotic map-based features—which capture nonlinear dynamics more effectively than traditional spectral features—with a data-driven OCS method. This dual innovation allows us to achieve superior accuracy (100%) while optimizing computational efficiency.

In the previous study, we introduced the Chebyshev Chaotic Map to create the phase space of DASPS data. While Chebyshev's chaotic maps have demonstrated excellent properties in cryptography and secure communications [41,44-46], their application to biomedical signal processing - and particularly EEG analysis - remains unexplored. The study introduced, for the first time, the use of Chebyshev's polynomials for EEG feature extraction in mental state classification. The map's superior ergodicity and more random output compared to conventional chaotic mappings (e.g., Logistic, Henon) [47] make it particularly suitable for capturing the nonlinear dynamics of anxiety-related brain activity. Then, we extracted two indicators from it: 1) the maximum density and 2) the corresponding sample. The features are then analyzed in 5 ways, including 1) feature 1 mapping from all channels using principal component analysis (PCA), 2) feature 1 from all channels, 3) feature 2 mapping from all channels using PCA, 4) feature 2 of all channels, and 5) each feature of each channel separately. The features were applied to the K-NN and SVM classifiers. Finally, classifiers were able to achieve an accuracy of 93.75% and 96.15% for classifying anxiety into two and four levels [20]. In the mentioned study, the feature was extracted from all the channels, and no method was used to select the optimal channel. The reason for using Optimal Channel Selection (OCS) algorithms is that by using such methods, computational costs are reduced, faster access to results is possible, classification accuracy is increased, and the focus on the channel that contains more information is increased [22]. As a result of the stated benefits, we decided to adopt a method for optimal channel selection in the present study and choose only one channel for each person out of 14 channels. To achieve this goal, we used some methods for channel selection containing 1) the minimum value of the Coefficient of Variation (CV) for each channel, 2) the minimum value of the CV related to the difference of both symmetrical channels, 3) the maximum value of the relative power for each channel, and 4) the maximum value of the relative power related to the difference of both symmetrical channels. Then, we used the phase space called the Chebyshev chaotic map, which was also used in the previous study [20]. To quantify the map, we used the density of points. Finally, we used K-NN and SVM classifiers to detect two and four levels of anxiety in four modes, including (1) features extracted from the selected channel using the first method, (2) features extracted from the selected channel using the second method, (3) features extracted from the selected channel using the third method and (4) features extracted from the selected channel using the fourth method.

2. Materials and Methods

This research used the preprocessed EEGs of the DASPS database. The data were collected from 23 people, who had no mental illness, including 13 women and 10 men, with an average age of 30 years, using the Emotive EPOC headset [11]. Emotive EPOC has 14 channels and two reference electrodes, situated according to the 10/20 International System in the locations of AF3, F7, F3, FC5, T7, P7, O1, O2, P8, T8, FC6, F4, F8, and AF4 [23] as shown in Figure 1. The sampling frequency was 128 Hz [24]. Signal quality was maintained by keeping impedance below 7 kΩ throughout recordings.

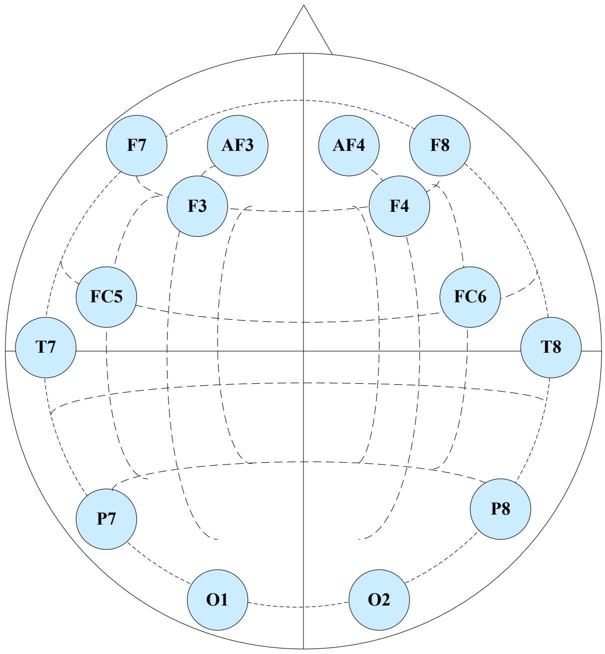

Figure 1. Sensor appointment of the 14 channels in the Emotiv EPOC according to the 10/20 International System

Note- While the dataset [11] describes this layout as conforming to the 10-20

International System, some electrode positions (e.g., FC5, FC6, AF3, AF4) are more precisely defined in the extended 10-10 system

The preprocessing pipeline applied to these data consisted of a multi-stage approach. First, an FIR bandpass filter (4–45 Hz) was implemented to attenuate low-frequency noise such as baseline drift and slow ocular activity, as well as high-frequency artifacts including muscle activity and environmental interference. Subsequently, artifact removal was performed using EEGLAB's AAR toolbox, which incorporated two key steps: ocular artifacts (EOG) were addressed via the BSSCCA method with a fractal dimension criterion (eog_fd) to identify and remove low-frequency components, while muscle artifacts (EMG) were mitigated using the iWASOBI (an asymptotically optimal Blind Source Separation (BSS) algorithm for autoregressive (AR) sources) algorithm combined with power spectral density analysis (emg_psd) to isolate high-energy components in the EMG frequency range. The entire preprocessing workflow was automated through scripting to ensure consistency across all recordings in the database [11].

The recording protocol is shown in Figure 2. The recording protocol followed strict experimental conditions as described in the original reference.

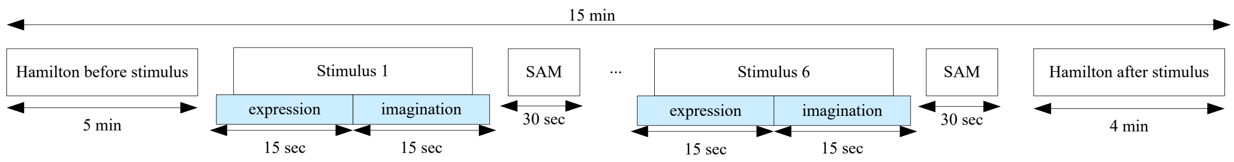

Figure 2. Protocol of anxiety stimulation

Participants were prepared for EEG recording in a controlled environment where they were instructed to keep their eyes closed and minimize movement during sessions. Flooding was used to induce anxiety in individuals. Then, six situations were selected in which individuals had the highest anxiety level. The situations include loss, family issues, financial topics, deadlines, witnessing a deadly accident, and mistreatment. The positions were read to the person by the psychotherapist for 15 seconds, one-to-one. Then, they were given 15 seconds to recall the situation. In the next step, individuals must rate their valence and arousal by a nine-point Self-Assessment Manikin (SAM) test, where valence was graded from negative to positive and arousal was graded from calm to exciting. Using the scores, the data were divided into different levels of anxiety. The division included four categories of normal, light, moderate, and severe anxiety or two levels of normal and anxiety, as shown in Figure 3. At the end of the experiment, to ensure its correctness, the anxiety level was re-measured by Hamilton Anxiety Rating Scale (HAM-A), with trained psychotherapists administering the evaluation. Finally, 136 ’Normal’ trials, 26 ’Light’ trials, 26 ’ Moderate’ trials, and 88 ’Severe’ trials were labeled, based on the combined SAM and HAM-A assessments [11].

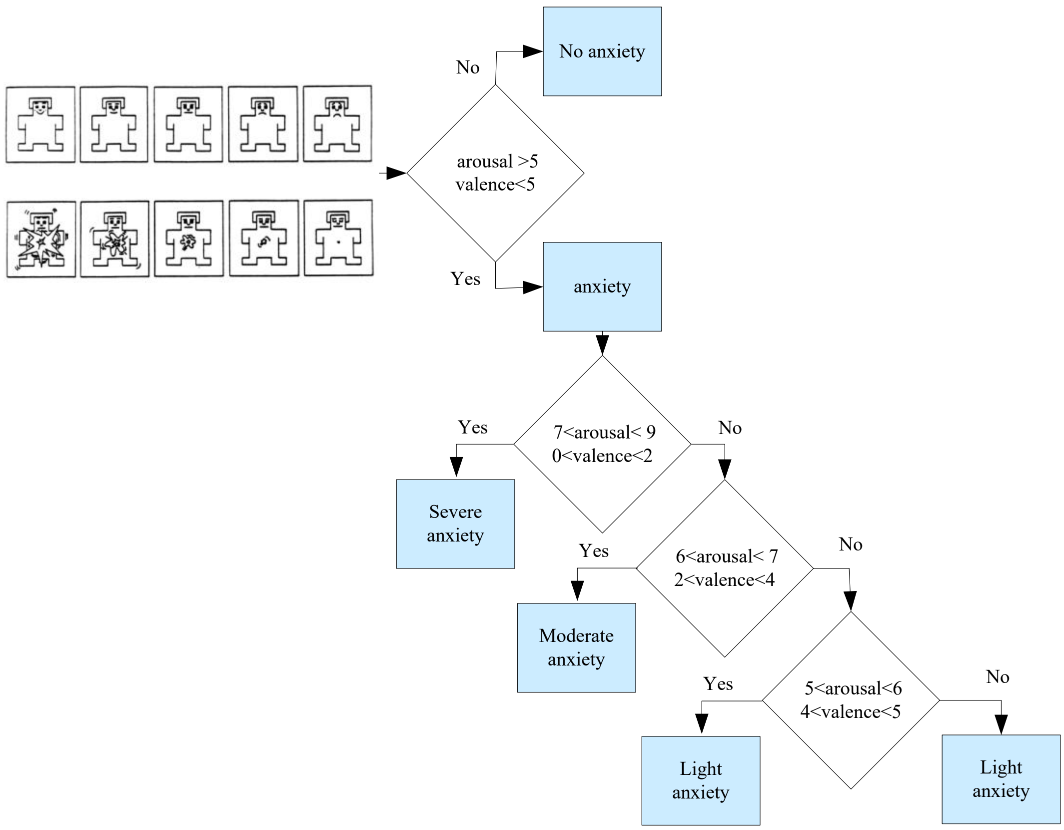

Figure 3. The process of dividing data into different levels of anxiety

2.1. Channel Selection

Using a method to select the optimal channel causes unnecessary channels to be removed without much change in the classification results. Also, the use of such algorithms allows us to better understand which brain channel is more related to the corresponding class [25]. The use of channel selection algorithms reduces the calculation time and increases the classification accuracy in most cases [26]. In past studies, different methods have been used to select the channel, which include spatiotemporal-filtering-based channel selection (STECS) [27], Fisher score [28], Recursive Channel Elimination (RCE) [25], and Variance [29]. In the presented study, methods based on the Coefficient of variation (CV) and Relative Power (RP) have been used, which are as follows:

1) The first method (M1):

In the first adopted method, the CV of each of the 14 channels was calculated for each subject. Then, a comparison was made between the values obtained from each channel, and the channel with the lowest value was selected as the optimal channel.

2) The second method (M2)

In the second channel selection method, first, the difference of symmetrical channels was calculated, which are as follows: AF3 and AF4, F7 and F8, F3 and F4, FC5 and FC6, T7 and T8, P7 and P8, O1, and O2; as it is known, seven pairs are obtained. Then, in each of the obtained differences, we calculated the CV. Finally, by comparing the CV values, we considered the minimum value as the selected symmetrical difference.

3) The third method (M3):

In this method, the RP of each of the 14 channels was calculated. Then we compared the relative power values and selected the channel with the maximum relative power value as the optimal channel.

4) Fourth method (M4):

In this method, the RP of the difference of symmetrical channels was calculated. Then the RP values were compared, and the maximum value was selected.

The CV-based approach prioritized channels with minimal signal variability, as high CV values (indicating instability or noise) were deemed unsuitable for reliable feature extraction. Similarly, the RP method emphasized channels with maximal relative power, reflecting heightened oscillatory activity that may correlate with anxiety-related neural dynamics. The use of symmetrical channel pairs (e.g., AF3-AF4, F7-F8) was motivated by evidence that hemispheric differences in EEG power may reflect anxiety-related lateralized neural activity.

2.1.1. Coefficient of Variation

CV, which is also considered as "relative standard deviation," is used to evaluate the variability of a sum relative to the standard deviation and is expressed as a percentage. The following formula can be used to obtain this criterion (Equation 1) [30]:

$$CV = \frac{std\ (x)}{mean\ (x)} \tag{1}$$

In this study, x is the signal string of each channel or the difference between both symmetrical channels. Since the high coefficient of variation is considered a weakness [31] and it indicates the data is out of control and is considered meaningless [32], we considered the minimum value of CV to select the optimal channel.

2.1.2. Relative Power (RP)

This criterion is also obtained using the following formula (Equation 2):

$$RP = \frac{\sum_{i=1}^{N}\left(S_x(i)\right)^2}{\sum_{x=1}^{M}\sum_{i=1}^{N}\left(S_x(i)\right)^2} \tag{2}$$

Here, M denotes the total number of signal components: M = 7 for differential signals (symmetrical pairs) and M = 14 for individual channels. x is the signal corresponding to each channel, or the signal corresponding to the difference between the symmetrical channels. In this formula, the denominator is fixed (one number related to each channel and one number related to differential mode), but the numerator is variable. N variable is proportional to the length of the signal, which is 1920 in all channels. Unlike M1, in which M was considered equal to 14, in this case, due to the difference in symmetrical electrodes, M is equal to 7. The best channel selected using this method is the channel with the highest relative power value. The denominator sums the squared signal values across all components, while the numerator is specific to the channel(s) under evaluation. The proposed channel selection method is shown in Figure 4.

2.2. Normalization

No preprocessing was performed on the EEG, except normalization. It is a linear transformation technique to normalize data in the range of [0, 1]. Considering the lower (min (xi)) and upper (max (xi)) values of data (xi), the normalized EEG is given by (Equation 3):

$$\hat{x}_i = \frac{x_i - \min(x_i)}{\max(x_i) - \min(x_i)} \tag{3}$$

Linear scaling is a special mode of min-max normalization where max $\hat{x}_i = 1$ and min $\hat{x}_i = 0$ [33]. The following formula is used to change the data range to ±1 (Equation 4):

$$x_{new} = \hat{x}_i \times 2 - 1 \tag{4}$$

In this case, the max $x_{new} = +1$ and the min $x_{new} = -1$, which is under the desired range of Chebyshev's Chaotic Map.

2.3. Feature Extraction

Phase Space Reconstruction (PSR) is a useful instrument for determining any low- or high-dimensional dynamic system [34]. A momentary state of such a system becomes a point in the phase space [35]. For a time series (X_i), where i= 1, 2, …, N, phase space is reconstructed using the following Equation 5:

$$Y_j = (X_j, X_{j+\tau}, X_{j+2\tau}, \dots, X_{j+(m-1)\tau}) \tag{5}$$

Where j= 1, 2, …, N-(m-1)τ. τ is the delay time, and m is the phase space dimension [34]. Phase space examines the hidden properties of the signal by hiding time [36]. The phase space of EEG contains good information about its dynamics and transitions [37]. The phase space features can help to improve the classification results [38, 39]. The most common method for phase space reconstruction is the Poincaré plot [36, 37]. Other methods such as 2D and 3D PSR

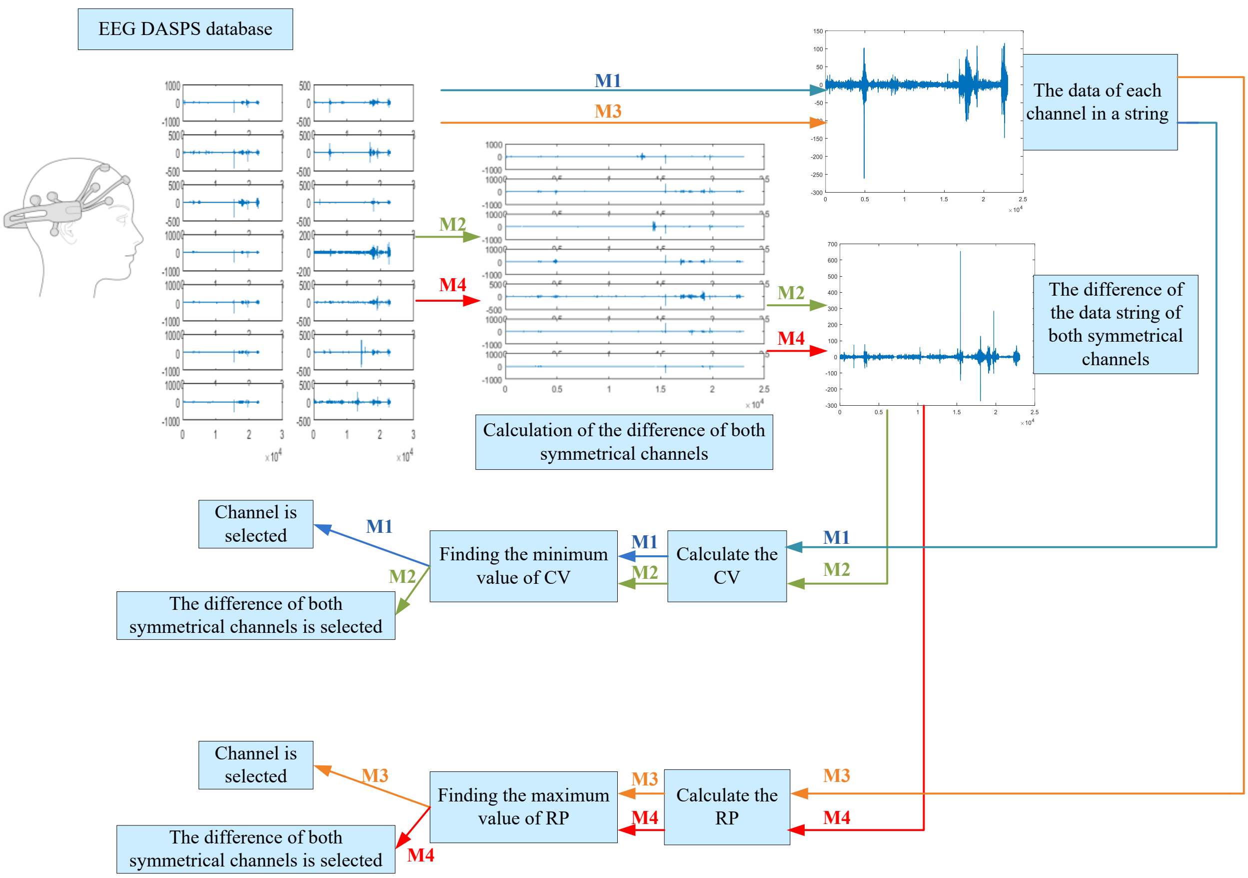

Figure 4. Channel selection process

[40], Autoregressive in Phase Space (ARPS), and amplitude-frequency analysis in phase space (AFAPS) [38] have also been used in previous studies. In our previous study, we used the Chebyshev chaotic map for the first time and obtained the phase space related to the EEG signal, and used a method based on the density of points to quantify this map [20], which is as follows:

2.3.1. Chebyshev's Chaotic Maps

Chaotic maps have a nonlinear structure [41]. Chebyshev's map is a 1D-chaotic plot [42]. It is used to avoid trapping in local optima and betterment the rummage [43]. Chebyshev's polynomials satisfy important specs, including the semigroup and the chaotic property [44, 45].

Chebyshev's polynomial $T_n(y)$ is a polynomial in the type of y with degree n [43] that n ϵ Z, yϵ [-1,1] and $T_n(y)$:[-1,1] → [-1,1]. The Chebyshev's polynomial is defined as (Equation 6):

$$T_n\,(y) = \cos(n.\arccos(x)) \tag{6}$$

where the trigonometric function $\cos(x)$ and $\arccos(x)$ are defined as cos(x): R → [0,π] and arccos(x):[-1,1] → [0,π] [44], n shows the sample number (ranging from 1 to 1920). X is also the normalized value of the sample at any point in the brain signal.

This mapping has been used to extract features in various fields, including public key cryptography [45], wireless body area networks [44], authentication protocols [41], and secure biometric-based authentication Scheme [46]; however, it has not been used in biomedical signal analysis so far. We selected this mapping due to its superior ergodicity and more randomized output compared to Logistic, Henon, and Sin mappings [47].

The map was quantified using the following steps. First, it was divided into 128 strips parallel to the vertical axis. Then, the density of points in each bar was calculated. We determine data density at each strip as the reciprocal of the sum of squared distances from each point, adding a fudge factor to prevent points actually within the strip from going to infinity [48]. Finally, two indicators, including (1) the maximum data density of all strips and (2) the sample where the maximum density occurred, were calculated [20]. These two indicators are shown in Figure 5. The feature vector for the selected channel was obtained (2×1 = 2, attribute × selected channels = the total number of features).

Table 2 provides the pseudo-code for the explanation of the map and its quantification.

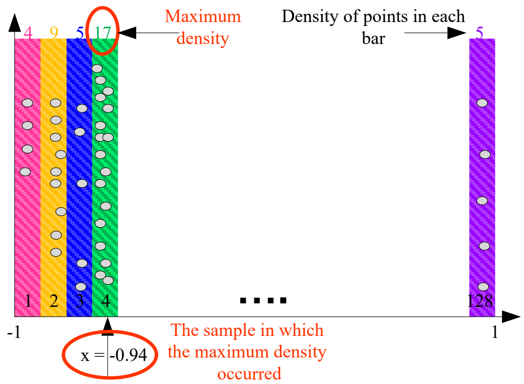

Figure 5. The proposed indicators for quantifying Chebyshev's chaotic map

2.4. Classification

One vs. all was used to label the data. Furthermore, K-fold cross-validation (K-CV) was used to divide the data into two categories of training and validation. The data are divided into K subsets [49]. The K-1 subsets are used as training sets, and one subset is used as a validation set. The process is repeated K times to include all subsets in the validation set [50]. We considered the value of K to be variable (2, 5, and 10). Two classifiers, including SVM and K-NN, were implemented for classification. The SVM implementation utilized a radial basis function kernel with automatic kernel scaling, which dynamically adjusts the kernel parameter based on the input feature space. This approach provides flexibility in handling both linear and nonlinear decision boundaries while maintaining computational efficiency. For the regularization parameter, we employed the default value of unity. For K-NN, the number of neighbors was systematically evaluated across integer values ranging from two to eight to determine the optimal neighborhood size. The distance metric employed was the Minkowski distance, which generalizes both Euclidean and Manhattan distances, with the exponent parameter set to its default value of two, corresponding to standard Euclidean distance. The

Table 2. A Pseudo-Code for Chebyshev Chaotic Map Quantification

Input:

- Input: X (normalized EEG signal) ($X \in [-1,1]$),
- n (sample number) (integer, n=1,2,…, 1920).
- ϵ: Small constant (e.g., ϵ=10−6) to avoid division by zero.

Output:

- Feature vector: [max_density,max_density_sample].

Steps:

1. **Generate Chebyshev Map**
   - ➢ *y = cos(n .* acos(X)); % Eq. 6: Chebyshev polynomial mapping*
   - This produces a chaotic map y= {y1, y2, …, yN}
2. **Divide the X-Axis into 128 Strips**
   - Partition the range [−1,1] into 128 equally spaced intervals (strips) along the *X*-axis.
   - ➢ *num_strips = 128;*
   - ➢ *strip_edges = linspace(-1, 1, num_strips + 1); % Divide x-axis (X ∈ [-1,1])*
3. **Calculate Density for Each Strip**
   - ➢ *density = zeros(num_strips, 1); % Initialize density array*
   - ➢ *for k = 1:num_strips*
   - ➢ *% Identify points in the k-th strip (X-range)*
   - ➢ *in_strip = (X >= strip_edges(k)) & (X < strip_edges(k+1));*
   - ➢ *y_in_strip = y(in_strip); % Corresponding y-values*
   - ➢ *% Calculate the density for the strip*
   - ➢ *sum_sq_dist = sum((y_in_strip - mean(y_in_strip)).^2) + ε;*
   - ➢ *density(k) = 1 / sum_sq_dist; % Density = reciprocal of squared distances*
   - ➢ *end*
4. **Extract Features**
   - ➢ *% Find the strip with maximum density*
   - ➢ *[max_density, max_strip] = max(density);*
   - ➢ *% Identify the sample index where max density occurs*
   - ➢ *samples_in_max_strip = find(X >= strip_edges(max_strip) & X < strip_edges(max_strip+1));*
   - ➢ *max_density_sample = samples_in_max_strip(1); % First sample in the strip*
5. **Return Feature Vector**
   - Combine results:
   - ➢ *features=[max_density,max_density_sample]*

nearest neighbor search method implemented an exhaustive search strategy to ensure accurate distance calculations across all training samples. These parameter choices reflect established practices in physiological signal analysis and provide a balanced approach between model complexity and generalization performance. The performance of the classification module was evaluated using accuracy and specificity. These measures are calculated using the confusion matrix shown in Table 3 using the following formulas [51]:

$$accuracy = \frac{TP + TN}{TP + TN + FP + FN} \quad (7)$$

$$specificity = \frac{TN}{TN + FP} \quad (8)$$

Figure 6 schematically illustrates the proposed framework.

3. Results

Table 3 shows nominated channels using the proposed channel selection methods.

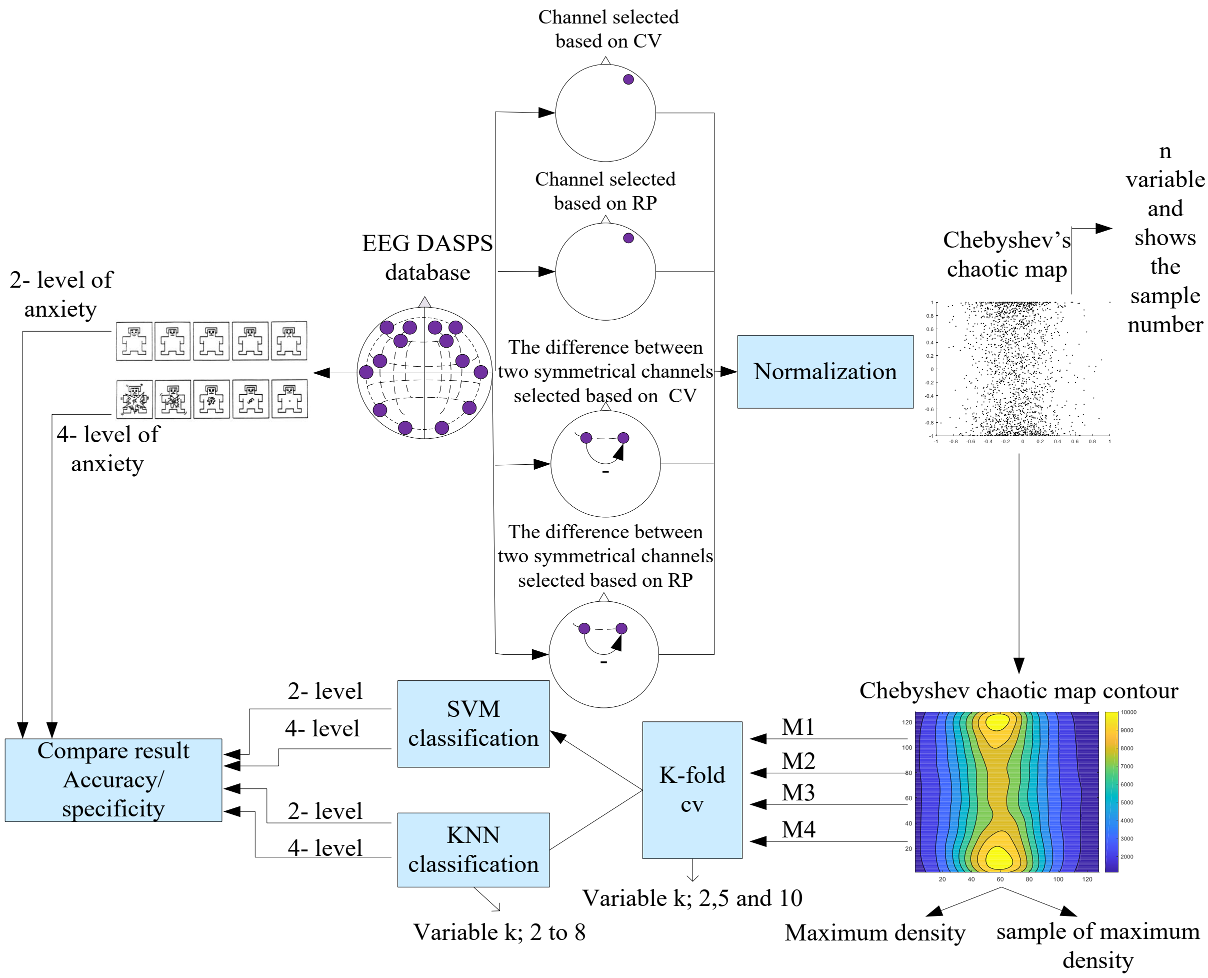

Figure 6. The proposed methodology

Table 3. Selected channels

Number of subject	M1	M2	M3	M4
1	AF4	F7 - F8	AF4	AF3 - AF4
2	T7	FC5 - FC6	T8	T7 - T8
3	T7	P7 - P8	O2	P7 - P8
4	T7	P7 - P8	O1	P7 - P8
5	F3	F7 - F8	AF4	AF3 - AF4
6	T7	F7 - F8	AF4	F7 - F8
7	T7	P7 - P8	O2	P7 - P8
8	F4	F7 - F8	O2	F7 - F8
9	FC6	F7 - F8	AF4	F7 - F8
10	AF3	F7 - F8	F7	F7 - F8
11	AF3	F7 - F8	F7	F7 - F8
12	AF3	P7 - P8	T8	P7 - P8
13	FC5	P7 - P8	AF4	AF3 - AF4
14	T7	F7 - F8	O2	O1 - O2
15	AF3	P7 - P8	O2	O1 - O2
16	F3	F7 - F8	O1	O1 - O2
17	T8	FC5 - FC6	F4	F3 - F4
18	F3	P7 - P8	AF4	AF3 - AF4
19	O1	FC5 - FC6	FC5	FC5 - FC6
20	T7	P7 - P8	T8	T7 - T8
21	AF3	F7 - F8	T8	F7 - F8
22	O1	F7 - F8	F8	F7 - F8
23	O1	F7 - F8	O1	F7 - F8

According to Table 3, the channels selected using the obtained methods are different. In the following, the channels and the differences between symmetrical channels that are selected more than other channels in different ways are described. Using the M1 method, the T7 channel is selected for 43.30% of participants. Using the M2 method, the difference between F7 and F8 channels was selected for 52.17% of individuals. In the M3 method, the AF4 channel was selected for 26.02% of people. Also, in the M4 method, the difference between F7 and F8 symmetrical channels was selected for 34.78% of subjects.

Tables 4, 5, 6, and 7 show the classification results of the M1, M2, M3, and M4, respectively. In each table, first the K-NN results, and then the SVM results are displayed.

Table 4. Best results for the M1 method of channel selection

Anxiety levels		**2-level**	**4-level**			
			1: Normal	**2: light anxiety**	**3: Moderate anxiety**	**4: severe anxiety**
K-NN						
(k for K-NN, k for k-fold)		(7,10) & (6,10)	(7,10)	(5,10)	(5,10)	(5,10)
Max	Accuracy	100 100	85.71	92.59	92.59	77.27
	Specificity	100 93.75	92.85	92.59	92.59	72
SVM						
k for k-fold		10	10	10	10	10
Max	Accuracy	70.37	62.96	92.59	92.59	77.77
	Specificity	80	60	92.59	92.59	75

Table 5. Best results for the M2 method of channel selection

Anxiety levels		**2-level**	**4-level**			
			1: Normal	**2: light anxiety**	**3: Moderate anxiety**	**4: severe anxiety**
K-NN						
(k for K-NN , k for k-fold)		(7,10)	(7,10)	(5,10)	(5,10)	(5,10)
Max	Accuracy	93.75	78.57	92.59	92.59	76.47
	Specificity	81.25	78.57	92.59	92.59	70
SVM						
k for k-fold		5	10	10	10	10
Max	Accuracy	66.07	67.85	92.59	92.59	74.07
	Specificity	72.72	64.70	92.59	92.59	73.91

The results of the four Tables revealed that comparing the K-NN and SVM, the maximum accuracy for all anxiety levels is higher for the K-NN classifier than that of the SVM. Also, according to the results in the above tables, we conclude that the best results are obtained in a 10-fold CV. By comparing two Tables 3 and 4, we conclude that overall the accuracy of each channel is higher than the differential mode. By comparing two Tables 6 and 7, we also reach the same conclusion that the results of each channel are better and higher than the differential mode. By general comparison of Tables 4, 5, 6, and 7, we conclude that the selection of the channel with the M3 method has made the classifier perform the initial classification of different levels of anxiety with higher accuracy. Figure 7 visually summarizes the highest performance trends across different channel selection methods (M1–M4) and classification tasks (2-level vs. 4-level anxiety) utilizing K-NN. It has explicitly pointed out the most important observations (e.g., the high accuracy of K-NN with M1 to M4 methods for 2-level and 4-level classification) to guide the reader's interpretation of the data from Tables 5 to 8.

Table 6. Best results for the M3 method of channel selection

Anxiety levels		2-level	4-level			
			1: Normal	2: light anxiety	3: Moderate anxiety	4: severe anxiety
K-NN						
(k for K-NN, k for k-fold)		(7,10)	(7,10)	(2,10)	(5,10)	(4,10)
Max	Accuracy	100	92.85	96.29	92.59	100
	Specificity	87.5	78.57	92.85	92.59	100
SVM						
k for k-fold		10	10	10	10	5
Max	Accuracy	62.96	62.96	92.59	92.59	70.90
	Specificity	60	64.28	92.59	92.59	71.42

Table 7. Best results for the M4 method of channel selection

Anxiety levels		2-level	4-level			
			1: Normal	2: light anxiety	3: Moderate anxiety	4: severe anxiety
K-NN						
(k for K-NN, k for k-fold)		(6,10) (7,10)	(7,10)	(5,10)	(5,10)	(6,10)
Max	Accuracy	100 100	92.30	92.59	92.59	81.25
	Specificity	93.75 100	71.42	92.59	92.59	66.66
SVM						
k for k-fold		10	10	10	10	10
Max	Accuracy	71.42	59.25	92.59	92.59	75
	Specificity	100	60	92.59	92.59	75

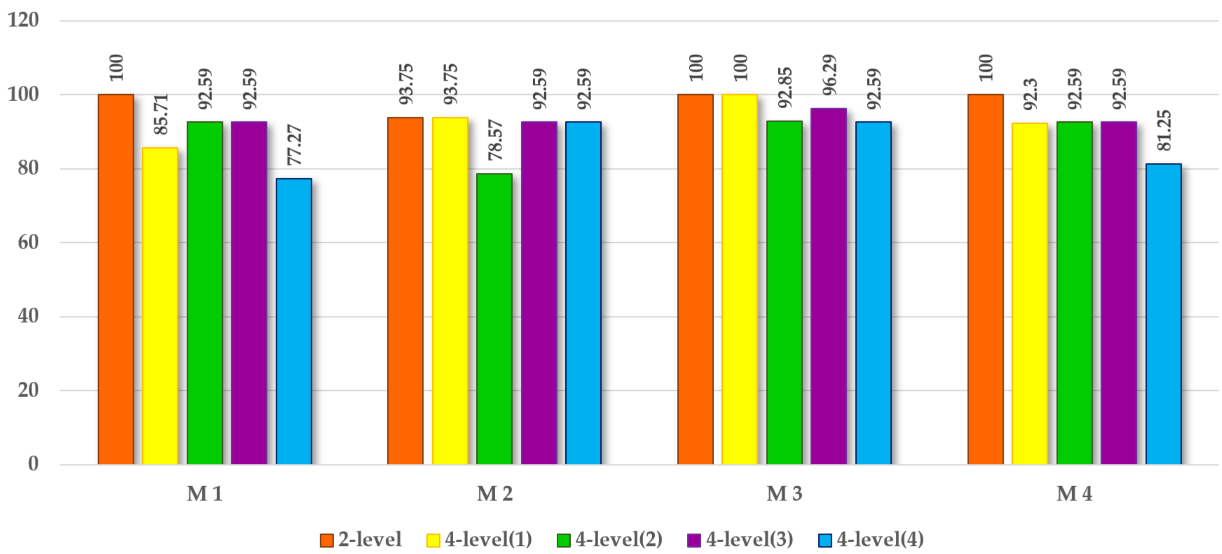

Figure 7. The highest K-NN accuracy rates across different channel selection methods (M1–M4) and classification tasks (2-level vs. 4-level anxiety)

Note- 1: Normal; 2: light anxiety; 3: Moderate anxiety; 4: severe anxiety is emphasized in parentheses for 4-level anxiety

4. Discussion

Anxiety is one of the most common psychiatric disorders that can be prevented and treated by timely diagnosis and treatment. The anxiety recognition system was presented using innovative features of the Chebyshev chaotic map. We also used methods for

Table 8. Overview of articles presented in the field of anxiety in terms of the number of data, analysis method, and results

Study	Number of data	Method of analysis	Best results
[10]	73	Temporal characteristics (IQR, MAD, SD, Mean, median, skewness, Trimmean) in 5 brain areas, including: FCP, LT, RT, F, and O, using paired-sample t-test and correlation analysis	-Higher MAD, Mean, Trimmean, SD, and IQR values in closed eye than those of open eye -Negative correlation of anxiety level with IQR, MAD, and SD in the open eye in the RT area -Positive relationship between anxiety level and SD in the closed eye in the FCP area
[11]	23 (DASPS)	Time domain, frequency amplitude, time-frequency amplitude, and quantitative measures, K-NN, SVM, SSAE	Accuracy for two classes: 83.50% Accuracy for four classes: 74.60% by SSAE
[12]	76	Measuring anxiety by TAS- Welch algorithm, spectral power analysis, TBR extraction- ANOVA, and Spearman	- TAS before the test had a significant positive correlation with parietal TBR - People with high test anxiety had higher TBR
[13]	119	Global connectivity in 6 frequency bands - SVR was used to investigate the relationship between the features and depression/anxiety	Positive and significant correlation of depression and anxiety with the alpha-2 band
[14]	23 (DASPS)	Fractal dimensions, Lyapunov exponent, approximate entropy- MRMR- MLP	Precision: 92.75%
[15]	45	MNI, orthogonalization, Gilbert deformation, seed method, The effect of depression, anxiety, and rumination scores on DMN and TPN using regression	-Relationship between depressive symptom scores and rumination scores (DMN> TPN) -Relationship between depression scores and anxiety scores (DMN <TPN) in the anterior cortex
[17]	81	PSD, FE, PLI- ANOVA- SVM, BP_Bagging, RF	-Accuracy: 97.83%
[18]	88	Fuzzy Entropy- LDA, K-NN, SVM, NBC, DT	-Accuracy: 86.93%
[19]	23 (DASPS)	Channel selection- asymmetry index, rational asymmetry, and mean power- wrapper method- DT, K-NN, SVM, MLP, RF	Accuracy: 94.90% (two-level anxiety) 92.74% (four-level anxiety)
[68]	32	Feature Extraction from Sensor Level, CfsSubsetEval, NBTree	Precision: 93.75%
[69]	20	Proximity matrix obtained by PLI, CNN	Accuracy: 67.67%
[70]	23 (DASPS)	Rhythm-specific multi-channel convolutional neural network for low/high arousal classification (CV: trial-independent)	Accuracy: 57.14%
[71]	23 (DASPS)	azimuthal projection-based 2D images and convolutional neural networks	Accuracy: 93%
[19]	23 (DASPS)	Channel selection, frequency domain features, including mean power, rational asymmetry, and asymmetry index, feature selection, Random Forest	Accuracy: 94.90% for two-level anxiety 92.74% for four-level anxiety
[58]	23 (DASPS)	Multiple filtration methods, features from the time, frequency, and time-frequency domains, SMOTE before classifying, KNN, SVM, and decision tree	Accuracy: 89.5%
[72]	23 (DASPS)	Spatio-temporal transition-based features, K-NN (5-fold CV)	Accuracy: 83.8%
Current study	23 (DASPS)	Channel selection- Chebyshev’s chaotic map-based features- SVM and K-NN	Accuracy: 100% (two-level anxiety) 100% (four-level anxiety)

channel selection. The attributes were applied to the K-NN and SVM classifiers. Our results showed the highest accuracy of 100% for both two/four-level anxiety recognition.

Table 8 provides an overview of the articles that have been done in this area. Accurate evaluation of articles indicates their inconsistency in various ways.

The present study examined data from DASPS [11]. There was no standard database with the same protocol for method evaluation. The data selection was not the same in the literature. Most of them focused on data collection. The data were dissimilar in sample number, electrode location, anxiety induction protocol, participants'/environmental conditions, and recording devices. Specifically, the number of samples varied between 23 [11] and 119 [13] participants.

An overview of multiple studies analyzing anxiety classification using the DASPS dataset shares the same sample size of 23 participants. The studies employ a variety of methods, including traditional machine learning techniques such as K-NN, SVM, and Random Forest, as well as deep learning approaches like CNNs and sparse autoencoders. Most rely on conventional feature extraction methods, including time-frequency analysis, asymmetry indices, entropy measures, and channel selection, with the highest reported accuracies reaching 94.9% for binary classification and 92.74% for four-class anxiety detection. Some studies, such as Mane's work [71] using azimuthal projection-based CNNs, achieve strong performance (93%), while others, like Maheshwari's trial-independent CNN [70], struggle with generalization (57.14%). Only one study [58] explicitly addresses class imbalance using SMOTE, and feature selection techniques like MRMR and wrapper methods are commonly applied to improve model efficiency. In contrast, the current study introduces a novel approach by leveraging Chebyshev's chaotic map-based features combined with SVM and K-NN classifiers, achieving a perfect 100% accuracy for both binary and four-class anxiety classification. This result significantly outperforms all other methods listed in the table, including deep learning models and ensemble techniques. Unlike some studies that rely on trial-dependent validation, this method demonstrates robust generalization without requiring data balancing techniques like SMOTE. The simplicity of using SVM and K-NN, rather than deep neural networks, further highlights the importance of advanced feature extraction over model complexity when working with smaller EEG datasets. The key distinction of this study lies in its unique feature representation, which appears to encode anxiety-related patterns more discriminatively than traditional time-frequency or asymmetry-based features. While deep learning methods like CNNs can achieve high accuracy, they often require extensive tuning and may overfit on limited data, as seen in Maheshwari's results. In comparison, the chaotic map-based approach provides a computationally efficient yet highly accurate alternative.

In the previous study [14], we used common nonlinear methods to extract features. But in another study [20], we investigated the innovative method of the Chebyshev chaotic map and used this map to transfer data to the phase space and extracted two indices from it for quantification. Finally, with the comparison between the two studies [14] and [20], we came to the conclusion that the use of the Chebyshev chaotic map, compared to other methods used in [14], has led to more acceptable results and higher accuracy. But in the mentioned study [20], no method was used to select the optimal channel. As a result, we conducted the current study to use methods to select the optimal channel and then use Chebyshev's chaotic map in those channels. Most previous experiments used temporal [10, 11], frequency [11], and time-frequency [11] properties of EEG in anxiety problems. Only a few studies have examined the chaotic features of the signal [14, 20]. Therefore, not much attention has been paid to nonlinear properties, especially phase space, which has only been investigated in our previous study [20].

Also, in terms of the channel selection algorithm, only two studies have used a method to select the optimal channel [16, 19]. In terms of channel selection approach, in [16, 19] study, t-test was used to classify anxiety into two levels and ANOVA was used to classify four levels. But in the current study, new approaches based on CV and RP have been used, and by using these methods, we can choose an optimal channel and achieve high results. According to the results obtained from the optimal channel selection, we conclude that in all methods, the channels in the frontal and temporal areas are selected more, which means that these areas provide information about anxiety. By comparing our study with other studies [16, 19], we conclude that our results were in line with their results in channel selection. That is, most of the channels selected by their method also included frontal and parietal channels. Our data-driven methods (CV and RP) identified specific channels and symmetrical pairs, which converge with neuroimaging and EEG biomarkers of anxiety. Frontal (e.g., AF3, AF4, F3, F4, F7, F8) and temporal (e.g., T7, T8) channels, which were frequently selected, align with prior neuroimaging studies implicating frontal-limbic networks in anxiety regulation. These dorsolateral prefrontal cortex (dlPFC) sites are implicated in emotion regulation and cognitive control. Dysregulation in dlPFC activity is linked to anxiety disorders [59], supporting their frequent selection across methods (e.g., subjects 10–12, 15, 21 for AF3 and subjects 1, 5, 6, 9, 13, and 18 for AF4).

Frontal asymmetry (F7-F8 differences in M2/M4) aligns with the "frontal alpha asymmetry" model, where right-lateralized activity correlates with withdrawal motivation and anxiety [60, 61]. This is consistent with prior EEG studies [62]. Temporal regions are associated with threat processing and arousal [63]. Nominated T7/T8 activity matches findings linking elevated temporal beta power to anxiety [64, 65]. Anxiety and depression are common mental illnesses that affect brain metabolism, especially in the frontal and temporal cortices [66]. Al-Qazzaz *et al.* (2019) found that frontal and temporal channels are consistently involved in the identification of different emotional states, including anxiety [67].

It evaluated SVM and K-NN with different structures. Besides, it examined different k values for the k-fold CV, unlike input vectors. Most studies have either focused on the statistical evaluation of the traits [10, 12, 13, 15] or have attempted to distinguish between anxious and non-anxious individuals [11, 14, 16, 19, 68, 69]. On the other hand, different learning algorithms and different classification evaluation criteria have also been reported in studies.

A maximum accuracy of 100% for recognizing light-level anxiety among four levels and 100% for separating two-level anxiety was achieved. Using a similar database, [11] a lower recognition rate was reported. Others achieved separation rates ranging from 67.67% to 97.83%. Compared to other studies, the classification performance was higher.

5. Conclusion

Classification of EEG signals into different levels of anxiety has recently become a challenging issue due to the human lifestyle. In this study, we tried to evaluate the EEG signal channels using several algorithms and select the optimal channels according to them. Then, we attempted to divide the EEG signal into different anxiety levels using Chebyshev's chaotic map. Specifically, two indices were extracted based on the data-point density. Finally, we used SVM and K-NN to classify different levels of anxiety. The scheme was evaluated using EEG recordings available in the DASPS dataset [11]. Using the proposed framework, the maximum accuracy rates were 100% for two-level and 100% for four-level anxiety detection. Additionally, it stressed the potential of some brain channels, as well as the important role of classifier structure in distinguishing anxiety levels. Our method's computational efficiency and reliance on frontal/temporal electrodes make it well-suited for real-time applications, such as integration with wearable EEG devices for continuous anxiety monitoring. The lightweight feature extraction (Chebyshev chaotic maps) and classification (SVM/K-NN) could enable embedded processing in portable systems, coupled with biofeedback interventions.

The following limitations of the study should be considered in the subsequent investigations. (1) The fruitfulness of Chebyshev's chaotic map measures should be evaluated using more data. (2) We extracted two simple features based on point density from the Chebyshev Chaotic Map. In future studies, other features can be used to quantify this map. (3) It classified four anxiety levels using the one vs. all strategy. The algorithm's performance should be evaluated in a multi-class classification problem. (4) The proposed measures are too simple, and their calculation is effortless and fast. Future studies should assess its effectiveness in diagnosing other neurological disorders. (5) In this study, only four-channel selection methods were used. In future studies, more effective methods can be used to select the optimal channel. (6) The performance of the proposed method may vary in noisy or clinical datasets where artifacts are more pronounced. Future works should explore integrating advanced preprocessing pipelines (e.g., wavelet denoising, deep learning-based artifact removal) to enhance signal fidelity. Besides, subsequent studies should evaluate the noise tolerance and adaptability of the framework. (7) While our within-subject design mitigates concerns about group-level demographic mismatches, exploring demographic influences in future studies will strengthen validity. (8) The observed 100% accuracy, while promising, may reflect the dataset's simplicity rather than true clinical robustness. Future research should focus on validating the approach in larger, diverse cohorts and naturalistic environments, while also exploring multimodal data integration and interpretability enhancements to facilitate clinical adoption.

Acknowledgments

The authors received no financial support for the research, authorship, and/or publication of this article.

Data availability statements: “This article examined the DASPS dataset [11], EEG signals, which are freely accessible in the public domain, available at the following URL: https://ieee-dataport.org/open-access/dasps-database”.

References

1- Julia Longworth and Jon Arcelus, "Prevalence of anxiety symptoms and disorders in the transgender population: A systematic review of the literature." (2016).

2- Yuan Liu *et al.*, "Anxiety and depression symptoms of medical staff under COVID-19 epidemic in China." *Journal of Affective Disorders,* Vol. 278pp. 144-48, (2021).

3- Eoin McElroy, Pasco Fearon, Jay Belsky, Peter Fonagy, and Praveetha Patalay, "Networks of depression and anxiety symptoms across development." *Journal of the American Academy of Child & Adolescent Psychiatry,* Vol. 57 (No. 12), pp. 964-73, (2018).

4- Johanna Özlem Schäfer, Eva Naumann, Emily Alexandra Holmes, Brunna Tuschen-Caffier, and Andrea Christiane Samson, "Emotion regulation strategies in depressive and anxiety symptoms in youth: A meta-analytic review." *Journal of youth and adolescence,* Vol. 46pp. 261-76, (2017).

5- Borwin Bandelow, Sophie Michaelis, and Dirk Wedekind, "Treatment of anxiety disorders." *Dialogues in clinical neuroscience,* Vol. 19 (No. 2), pp. 93-107, (2017).

6- Jessica A Michael, Michael Wang, Manreena Kaur, Paul B Fitzgerald, Bernadette M Fitzgibbon, and Kate E Hoy, "EEG correlates of attentional control in anxiety disorders: A systematic review of error-related negativity and correct-response negativity findings." *Journal of Affective Disorders,* Vol. 291pp. 140-53, (2021).

7- Borwin Bandelow and Sophie Michaelis, "Epidemiology of anxiety disorders in the 21st century." *Dialogues in clinical neuroscience,* Vol. 17 (No. 3), pp. 327-35, (2015).

8- Patrick E McKnight, Samuel S Monfort, Todd B Kashdan, Dan V Blalock, and Jenna M Calton, "Anxiety symptoms and functional impairment: A systematic review of the correlation between the two measures." *Clinical psychology review,* Vol. 45pp. 115-30, (2016).

9- Marianne Lucena da Silva, Rodrigo Santiago Barbosa Rocha, Mohamed Buheji, Haitham Jahrami, and Katiane da Costa Cunha, "A systematic review of the prevalence of anxiety symptoms during coronavirus epidemics." *Journal of Health Psychology,* Vol. 26 (No. 1), pp. 115-25, (2021).

10- Jingwen Li, Huangyanqiu Ran, and Jia Zhao, "Relationship Between Multiple Temporal Features of Resting EEG and the Anxiety State of Normal Subjects." in *2019 12th International Congress on Image and Signal Processing, BioMedical Engineering and Informatics (CISP-BMEI)*, (2019): *IEEE*, pp. 1-6.

11- Asma Baghdadi, Yassine Aribi, Rahma Fourati, Najla Halouani, Patrick Siarry, and Adel M Alimi, "Dasps: a database for anxious states based on a psychological stimulation." *arXiv preprint arXiv:1901.02942,* (2019).

12- Hua Wei, Lei Chang, Qiong Huang, and Renlai Zhou, "Relation between spontaneous electroencephalographic theta/beta power ratio and test anxiety." *Neuroscience Letters,* Vol. 737p. 135323, (2020).

13- Lucas R Trambaiolli and Claudinei E Biazoli, "Resting-state global EEG connectivity predicts depression and anxiety severity." in *2020 42nd Annual International Conference of the IEEE Engineering in Medicine & Biology Society (EMBC)*, (2020): *IEEE*, pp. 3707-10.

14- Faezeh Daneshmand-Bahman and Ateke Goshvarpour, "Classification of EEG Signals in Two Levels of Normal and Anxious Using Nonlinear." *Journal of Cognitive Psychology,* Vol. 9 (No. 3), (2021).

15- AV Bocharov, GG Knyazev, AN Savostyanov, AE Saprygin, EA Proshina, and SS Tamozhnikov, "Relationship of Depression, Anxiety, and Rumination Scores with EEG Connectivity of Resting State Networks." *Human Physiology,* Vol. 47 (No. 2), pp. 123-27, (2021).

16- Aamir Arsalan and Muhammad Majid, "A study on multi-class anxiety detection using wearable EEG headband." *Journal of Ambient Intelligence and Humanized Computing,* Vol. 13 (No. 12), pp. 5739-49, (2022).

17- Zhongxia Shen *et al.*, "Aberrated multidimensional EEG characteristics in patients with generalized anxiety disorder: a machine-learning based analysis framework." *Sensors,* Vol. 22 (No. 14), p. 5420, (2022).

18- Abdulhakim Al-Ezzi, Amal A Al-Shargabi, Fares Al-Shargie, and Ammar T Zahary, "Complexity analysis of EEG in patients with social anxiety disorder using fuzzy entropy and machine learning techniques." *IEEE Access,* Vol. 10pp. 39926-38, (2022).

19- Farah Muhammad and Saad Al-Ahmadi, "Human state anxiety classification framework using EEG signals in response to exposure therapy." *Plos one,* Vol. 17 (No. 3), p. e0265679, (2022).

20- Faezeh Daneshmand-Bahman and Ateke Goshvarpour, "A New EEG Processing Approach using the Chebyshev Chaotic Map: Application in Anxiety Classification." *Iranian Journal of Biomedical Engineering,* Vol. 16 (No. 2), pp. 115-31, (2022).

21- Malik Muhammad Naeem Mannan, Muhammad Ahmad Kamran, and Myung Yung Jeong, "Identification and removal of physiological artifacts from electroencephalogram signals: A review." *IEEE Access,* Vol. 6pp. 30630-52, (2018).

22- Luis Alfredo Moctezuma and Marta Molinas, "EEG channel-selection method for epileptic-seizure classification based on multi-objective optimization." *Frontiers in neuroscience,* Vol. 14p. 593, (2020).

23- Fernando Flórez, José Maria Azorín, Eduardo Iáñez, Andrés Úbeda, and Eduardo Fernández, "Development of a Low-cost SVM-based Spontaneous Brain-computer Interface." in *IJCCI (NCTA)*, (2011), pp. 415-21.

24- Rodrigo Ramele, Ana Julia Villar, and Juan Miguel Santos, "Epoc Emotiv EEG basics." *arXiv preprint arXiv:2206.09051,* (2022).

25- Michael Schröder *et al.*, "Robust EEG channel selection across subjects for brain-computer interfaces." *EURASIP Journal on Advances in Signal Processing,* Vol. 2005pp. 1-10, (2005).

26- Aleksandra Dura and Agnieszka Wosiak, "EEG channel selection strategy for deep learning in emotion recognition." *Procedia Computer Science,* Vol. 192pp. 2789-96, (2021).

27- Feifei Qi *et al.*, "Spatiotemporal-filtering-based channel selection for single-trial EEG classification." *IEEE Transactions on Cybernetics,* Vol. 51 (No. 2), pp. 558-67, (2020).

28- Yongkoo Park and Wonzoo Chung, "Optimal channel selection using correlation coefficient for CSP based EEG classification." *IEEE Access,* Vol. 8pp. 111514-21, (2020).

29- Athar A Ein Shoka, Monagi H Alkinani, AS El-Sherbeny, Ayman El-Sayed, and Mohamed M Dessouky, "Automated seizure diagnosis system based on feature extraction and channel selection using EEG signals." *Brain Informatics,* Vol. 8pp. 1-16, (2021).

30- JA Canchola, Sh Tang, P Hemyari, E Paxinos, and E Marins, "Correct use of percent coefficient of variation (% CV) formula for log-transformed data." *MOJ Proteom. Bioinform,* Vol. 6 (No. 4), (2017).

31- Carla Santos and Cristina Dias, "Note on the coefficient of variation properties." *Brazilian Electronic Journal of Mathematics,* Vol. 2 (No. 4), pp. 101-11, (2021).

32- Charles E Brown, Applied multivariate statistics in geohydrology and related sciences. *Springer Science & Business Media*, (2012).

33- Bikesh Kumar Singh, Kesari Verma, and AS Thoke, "Investigations on impact of feature normalization techniques on classifier's performance in breast tumor classification." *International Journal of Computer Applications,* Vol. 116 (No. 19), (2015).

34- Sang-Hong Lee, Joon S Lim, Jae-Kwon Kim, Junggi Yang, and Youngho Lee, "Classification of normal and epileptic seizure EEG signals using wavelet transform, phase-space reconstruction, and Euclidean distance." *Computer methods and programs in biomedicine,* Vol. 116 (No. 1), pp. 10-25, (2014).

35- RC Watt and SR Hameroff, "Phase space electroencephalography (EEG): a new mode of intraoperative EEG analysis." *International journal of clinical monitoring and computing,* Vol. 5pp. 3-13, (1988).

36- Zahra Barati Moghadam, Zahra Ghaemian, Najmeh Sahebalam, Ateke Goshvarpour, and Ghasem Sadeghi Bajestani, "Gender Differences in Cardiovascular Performance While Running at Maximum Heart Rate: Emphasis on Phase Space Dynamic." *Journal of Applied Exercise Physiology,* Vol. 16 (No. 31), pp. 71-87, (2020).

37- Morteza Zangeneh Soroush, Keivan Maghooli, Seyed Kamaledin Setarehdan, and Ali Motie Nasrabadi, "Emotion recognition through EEG phase space dynamics and Dempster-Shafer theory." *Medical Hypotheses,* Vol. 127pp. 34-45, (2019).

38- Yonghui Fang, Minyou Chen, and Xufei Zheng, "Extracting features from phase space of EEG signals in brain–computer interfaces." *Neurocomputing,* Vol. 151pp. 1477-85, (2015).

39- Minyou Chen, Yonghui Fang, and Xufei Zheng, "Phase space reconstruction for improving the classification of single trial EEG." *Biomedical Signal Processing and Control,* Vol. 11pp. 10-16, (2014).

40- Rajeev Sharma and Ram Bilas Pachori, "Classification of epileptic seizures in EEG signals based on phase space representation of intrinsic mode functions." *Expert*

Systems with Applications, Vol. 42 (No. 3), pp. 1106-17, (2015).

41- Dharminder Dharminder and Pratik Gupta, "Security analysis and application of Chebyshev Chaotic map in the authentication protocols." *International Journal of Computers and Applications,* Vol. 43 (No. 10), pp. 1095-103, (2021).

42- Fei Qi, Sijiang Huang, Tong Li, Haotian Yang, and Xuejing Kang, "2D henon-chebyshev chaotic map for image encryption." in *2019 IEEE 21st International Conference on High Performance Computing and Communications; IEEE 17th International Conference on Smart City; IEEE 5th International Conference on Data Science and Systems (HPCC/SmartCity/DSS)*, (2019): *IEEE*, pp. 774-81.

43- Ali Kaveh, R Mahdipour Moghanni, and SM Javadi, "Chaotic optimization algorithm for performance-based optimization design of composite moment frames." *Engineering with Computers,* Vol. 38 (No. 3), pp. 2729-41, (2022).

44- Gaimei Gao, Xinguang Peng, Ye Tian, and Zefeng Qin, "A chaotic maps-based authentication scheme for wireless body area networks." *International Journal of Distributed Sensor Networks,* Vol. 12 (No. 7), p. 2174720, (2016).

45- Chandrashekhar Meshram, Mohammad S Obaidat, and Sarita G Meshram, "Chebyshev chaotic map-based ID-based cryptographic model using subtree and fuzzy-entity data sharing for public key cryptography." *Security and Privacy,* Vol. 1 (No. 1), p. e12, (2018).

46- Santanu Chatterjee, Sandip Roy, Ashok Kumar Das, Samiran Chattopadhyay, Neeraj Kumar, and Athanasios V Vasilakos, "Secure biometric-based authentication scheme using Chebyshev chaotic map for multi-server environment." *IEEE Transactions on Dependable and Secure Computing,* Vol. 15 (No. 5), pp. 824-39, (2016).

47- Ali Shakiba, "Generating dynamical S-boxes using 1D Chebyshev chaotic maps." *Journal of Computing and Security,* Vol. 7 (No. 1), pp. 1-17, (2020).

48- Malcolm McLean. (2024). data density plot. [Online]. Available: http://www.mathworks.com/matlabcentral/fileexchange/31726-data-density-plot.

49- Yoshua Bengio and Yves Grandvalet, "No unbiased estimator of the variance of k-fold cross-validation." *Advances in Neural Information Processing Systems,* Vol. 16(2003).

50- Davide Anguita, Alessandro Ghio, Sandro Ridella, and Dario Sterpi, "K-Fold Cross Validation for Error Rate Estimate in Support Vector Machines." in *DMIN*, (2009), pp. 291-97.

51- Trent D Buskirk, Antje Kirchner, Adam Eck, and Curtis S Signorino, "An introduction to machine learning methods for survey researchers." *Survey Practice,* Vol. 11 (No. 1), (2018).

52- Jaime Salvador–Meneses, Zoila Ruiz–Chavez, and Jose Garcia–Rodriguez, "Compressed k NN: K-nearest neighbors with data compression." *Entropy,* Vol. 21 (No. 3), p. 234, (2019).

53- Muchammad Arfan Lusiandro, Surya Michrandi Nasution, and Casi Setianingsih, "Implementation of the advanced traffic management system using k-nearest neighbor algorithm." in *2020 International conference on information technology systems and innovation (ICITSI)*, (2020): *IEEE*, pp. 149-54.

54- Ahmed Alsaffar and Nazlia Omar, "Integrating a Lexicon based approach and K nearest neighbour for Malay sentiment analysis." *Journal of Computer Science,* Vol. 11 (No. 4), p. 639, (2015).

55- Renyuan Zhang and Siyang Cao, "Support vector machines for classification of automotive radar interference." in *2018 IEEE Radar Conference (RadarConf18)*, (2018): *IEEE*, pp. 0366-71.

56- Nick Guenther and Matthias Schonlau, "Support vector machines." *The Stata Journal,* Vol. 16 (No. 4), pp. 917-37, (2016).

57- Jinglin Xu, Junwei Han, Feiping Nie, and Xuelong Li, "Multi-view scaling support vector machines for classification and feature selection." *IEEE Transactions on Knowledge and Data Engineering,* Vol. 32 (No. 7), pp. 1419-30, (2019).

58- Syarifah Noor Syakiylla Sayed Daud, Rubita Sudirman, and Tee Wee Shing, "Safe-level SMOTE method for handling the class imbalanced problem in electroencephalography dataset of adult anxious state." *Biomedical Signal Processing and Control,* Vol. 83p. 104649, (2023).

59- Lauren K White, Walid Makhoul, Marta Teferi, Yvette I Sheline, and Nicholas L Balderston, "The role of dlPFC laterality in the expression and regulation of anxiety." *Neuropharmacology,* Vol. 224p. 109355, (2023).

60- Johannes Rodrigues, Mathias Müller, Andreas Mühlberger, and Johannes Hewig, "Mind the movement: Frontal asymmetry stands for behavioral motivation, bilateral frontal activation for behavior." *Psychophysiology,* Vol. 55 (No. 1), p. e12908, (2018).

61- Micayla French Lacey and Philip A Gable, "Frontal asymmetry as a neural correlate of motivational conflict." *Symmetry,* Vol. 14 (No. 3), p. 507, (2022).

62- Sarah Glier, Alana Campbell, Rachel Corr, Andrea Pelletier-Baldelli, and Aysenil Belger, "Individual differences in frontal alpha asymmetry moderate the relationship between acute stress responsivity and state and trait anxiety in adolescents." *Biological psychology,* Vol. 172p. 108357, (2022).

63- Dinavahi VPS Murty, Songtao Song, Srinivas Govinda Surampudi, and Luiz Pessoa, "Threat and reward imminence processing in the human brain." *Journal of Neuroscience,* Vol. 43 (No. 16), pp. 2973-87, (2023).

64- Hangwei Wang *et al.*, "The power spectrum and functional connectivity characteristics of resting-state EEG in patients with generalized anxiety disorder." *Scientific Reports,* Vol. 15 (No. 1), p. 5991, (2025).

65- Valdenilson Ribeiro Ribas *et al.*, "Padrão de ansiedade, insegurança, medo, pânico e/ou fobia observado no exame de eletroencefalografia quantitativa (QEEG)." *Dementia & Neuropsychologia,* Vol. 12pp. 264-71, (2018).

66- Xuenan Lang, Dan Wen, Qiqi Li, Qin Yin, Mingyu Wang, and Yong Xu, "fNIRS evaluation of frontal and temporal cortex activation by verbal fluency task and high-level cognition task for detecting anxiety and depression." *Frontiers in psychiatry,* Vol. 12p. 690121, (2021).

67- Noor Kamal Al-Qazzaz, Mohannad K Sabir, Sawal Ali, Siti Anom Ahmad, and Karl Grammer, "Effective EEG channels for emotion identification over the brain regions using differential evolution algorithm." in *2019 41st Annual International Conference of the IEEE Engineering in Medicine and Biology Society (EMBC)*, (2019): *IEEE*, pp. 4703-06.

68- Manousos A Klados, Niki Pandria, Alkinoos Athanasiou, and Panagiotis D Bamidis, "An automatic EEG based system for the recognition of math anxiety." in *2017 IEEE 30th International Symposium on Computer-Based Medical Systems (CBMS)*, (2017): *IEEE*, pp. 409-12.

69- Yunlong Xie *et al.*, "Anxiety and depression diagnosis method based on brain networks and convolutional neural networks." in *2020 42nd Annual International Conference of the IEEE Engineering in Medicine & Biology Society (EMBC)*, (2020): *IEEE*, pp. 1503-06.

70- Daksh Maheshwari, Samit Kumar Ghosh, RK Tripathy, Manish Sharma, and U Rajendra Acharya, "Automated accurate emotion recognition system using rhythm-specific deep convolutional neural network technique with multi-channel EEG signals." *Computers in Biology and Medicine,* Vol. 134p. 104428, (2021).

71- Swaymprabha Alias Megha Mane and Arundhati A Shinde, "Novel imaging approach for mental stress detection using EEG signals." in *Proceedings of Academia-Industry Consortium for Data Science: AICDS 2020*: *Springer*, (2022), pp. 25-36.

72- Debatri Chatterjee, Rahul Gavas, and Sanjoy Kumar Saha, "Detection of mental stress using novel spatio-temporal distribution of brain activations." *Biomedical Signal Processing and Control,* Vol. 82p. 104526, (2023).